

碱度对直流埋弧焊熔滴阶段电化学致氧的影响

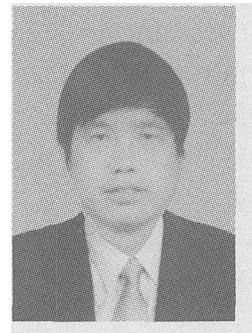
李晓泉^{1,2}, 杜则裕¹, 李云涛¹, 刘鹏飞², 王光耀²

(1. 天津大学, 天津 300072; 2. 江苏科技大学, 江苏 镇江 212003)

摘要: 采用试验室设计各种碱度烧结焊剂在两种极性条件下进行快速焊接提取激冷态熔滴金属, 应用 LECO 氧氮分析仪测定其氧氮含量, 以间接分析焊接电弧阴极和阳极熔渣/液态金属界面发生的冶金电化学作用。结果表明, 在焊丝末端熔滴生长阶段, 直流反极性条件下存在电化学增氧, 而直流正极性条件下则存在电化学脱氧。试验揭示出碱度对这种冶金电化学作用有着极为重要的影响, 随着碱度的增大, 受熔渣离子特性电极反应动力学的影响, 其产生的与热化学活性理论相反的电化学致氧效应愈加明显, 从而成为有必要加以考虑的冶金因素。

关键词: 碱度; 电化学反应; 埋弧焊

中图分类号: TG 445 文献标识码: A 文章编号: 0253-360X(2005)02-09-04



李晓泉

0 序 言

自 Tuliani^[1]等人建立起 IIW 碱度计算式以来, 碱度一直作为衡量焊接过程熔渣与液态金属冶金作用的一重要指标。通常认为, 高碱度可抑制熔渣对液态金属的热化学作用, 从而使焊缝金属获得低的氧含量。焊接实践表明, 即使采用碱度高达 2.5 的高碱度焊剂进行埋弧焊接, 所获得的焊缝金属氧含量也只能控制在 0.02% 左右, 与母材及焊丝金属通常的 0.002% 氧含量相比, 仍存在约 10 倍的增氧量。对于埋弧焊 SAW (Submerged arc welding) 这样一种伴随有强烈熔渣-液态金属交互作用的焊接方法, Lau^[2,3]等人的研究指出, 液态金属的增氧主要发生在熔滴阶段(包括焊丝尖端熔滴生长阶段及熔滴穿越弧柱的过渡阶段)。在此期间通过熔渣与液态金属界面热化学作用而增氧。随后, Blandar, Olson 等人^[4-11]根据近代熔渣的离子理论及共存理论, 又提出了在焊接电弧的阴阳两极——焊丝尖端及熔池边缘附近存在强烈电化学作用, 从而也对液态金属的增氧具有较大影响的观点, 并用试验证实了上述观点的客观性。考虑到电化学作用与热化学作用存在一些本质的区别, 如电化学作用只有在通有电流的情况下才能在阴阳两极分区进行, 这也意味着焊接过程焊缝金属的增氧机制同时存在热化学和电化学两种, 而碱度的概念却是仅基于熔渣的热化学活性而建立的。关于碱度对熔渣/液态金属界

面热化学作用的影响, 人们已有了较多的认识, 然而碱度对电化学作用的影响却是尚待研究的新课题, 可以预计, 对该问题的深入研究可进一步丰富、完善传统的焊接冶金理论。

1 直流焊接冶金电化学反应机理

根据液态熔渣中存在离子的观点, 在图 1 所示 SAW 直流反接 (DCEP) 及直流正接 (DCEN) 焊接示意图中, 焊丝末端熔滴与液态熔渣界面及熔池边缘熔渣与液态金属界面间, 由于界面存在特大的电流密度导致的电化学致氧变化为

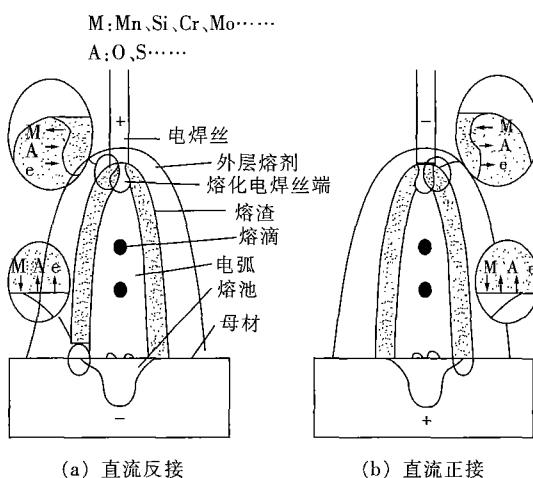
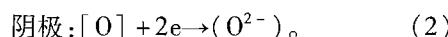
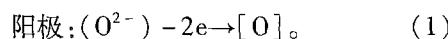


图 1 SAW 直流反接和直流正接电化学反应示意图

Fig. 1 Schematic diagram of electrochemical reaction in DCEP and DCEN



考虑到焊丝末端渣-金属界面较熔池边缘小得多,因此在直流反接情况下,生长期熔滴金属存在强烈的电化学增氧;而在直流正接情况下则存在强烈的电化学脱氧。当熔滴脱离焊丝穿越弧柱期间,由于熔滴与焊接回路断路,电化学作用停止,待进入熔池后,又进行与熔滴生长阶段逆向的电化学反应。

由上述分析可见,在直流焊接条件下,熔渣与液态金属界面除存在传统的热化学作用外,还存在一种特定的电化学作用。该冶金电化学作用必定对焊缝金属化学成分产生一定的影响。

2 试验方法

为研究碱度对熔滴阶段熔渣/液态金属界面电化学作用的影响,试验采用相同条件下直流正、反极性接法埋弧焊接快速提取激冷态熔滴的方法,以分析熔滴中电化学致氧的变化情况。具体过程为,在试验室按表 1 成分配制不同碱度(BI)的物料制成烧结焊剂,为获得激冷态熔滴,在尺寸为 224 mm × 119 mm × 12 mm 的铜板背面钎焊一盛水槽,并开设水冷循环进出口接管。焊接时配合 H08A, φ2 mm 焊丝,在接通冷却水的铜板上进行高速焊接,焊接参数为电流 $I = 360 \text{ A} \pm 5 \text{ A}$ 、电压 $U = 38 \text{ V} \pm 0.5 \text{ V}$ 、焊接速度 $v = 1.32 \text{ m/min}$ 。

表 1 试验室制作烧结焊剂成分(质量分数,%)

Table 1 Chemical compositions of agglomerated fluxes made in laboratory

编号	MgO	CaO	SiO ₂	碱度/BI(IIW)
L1	10	45	45	1.2
L2	20	40	40	1.5
L3	30	35	35	1.9
L4	40	30	30	2.3
L5	50	25	25	3.0

注:BI = [CaF₂ + CaO + MgO + 0.5(FeO + MnO)]/[SiO₂ + 0.5(Al₂O₃ + MnO)]

按上述方法试验,可在铜板上得到“冻结”有高温特性的无熔池球状激冷态熔滴(见图 2)。由于熔滴阶段包括熔滴生长期和熔滴过渡两个过程,但熔滴生长期从时间上讲是远大于熔滴过渡期时间的。根据 Blandar 等人的观点,在熔滴生长期同时存在热化学和电化学两种作用,熔滴过渡时,由于熔滴与

焊接回路不直接构成回路,因而电化学作用暂时停止,仅存在熔滴表面覆盖的熔渣与其发生热化学作用。之后分别将焊丝末端熔化熔滴与铜板上熔滴取下,用砂纸打磨干净并用有机溶剂清洗后在美国 LECO 氧氮分析仪上作其氧氮含量分析;熔滴的内部结构可用金相镶嵌法制成试样后在 JXA-840A 扫描电镜上观察。

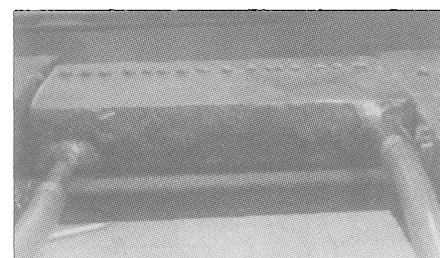


图 2 激冷态熔滴照片图

Fig. 2 Photographs of rapid cooled droplet

3 试验结果及分析

3.1 激冷态熔滴内部形貌特征

图 3 是几种试验焊剂焊接时所提取的熔滴内部扫描电镜照片。该图显示熔滴内部呈现完全奥氏体凝固组织,未发生二次相变。表明所提取的熔滴较好地“冻结”了高温奥氏体的某些特征,加之完全未形成熔池,因而为间接研究熔滴阶段的冶金行为提供了难得的条件。

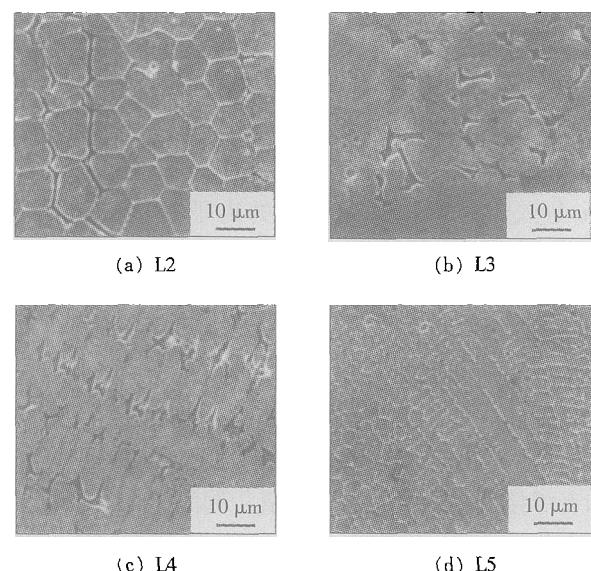
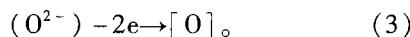


图 3 激冷态熔滴内部组织扫描电镜图

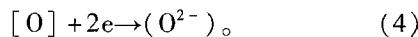
Fig. 3 SEM photographs of inside rapid cooled droplet

3.2 极性与熔滴金属氧含量的关系

图4、5分别为根据试验结果绘制的正、反极性焊接时焊丝末端生长期熔滴和铜板上取得的过渡熔滴氧含量随碱度变化的曲线。从图中可以看出,在同样条件下,直流反极性接法所提取得的熔滴金属氧含量总是高于正极性情形,而且随着碱度的增大,这种差异愈加明显。该现象完全从熔渣与熔滴金属热化学作用观点是难以解释的,但以电化学的观点却能得到较好的解释。根据 Blandar 等人的研究,在 SAW 电弧的阳极,由于熔融熔渣的分流效应,在熔渣与液态熔滴界面存在电极反应



而在焊接电弧的阴极,则存在上述逆电极反应



电化学作用的结果导致直流反极性(DCEP)时,焊丝尖端熔滴生长阶段增氧,而在直流正极性(DCEN)时则脱氧,因而出现图4、5所示的直流反极性接法时熔滴金属氧含量总是高于正极性的情形。这与 Blandar 等人的试验结果是完全吻合的,同时该试验结果也再次支持了 Blandar 的电化学观点。

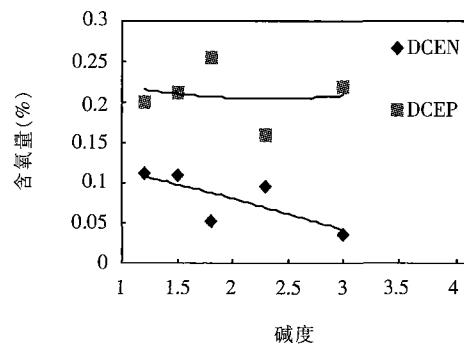


图4 直流正反接时生长期熔滴氧含量随碱度变化曲线

Fig.4 Oxygen content curves in growing droplet with basicity index in DCEN and DCEP

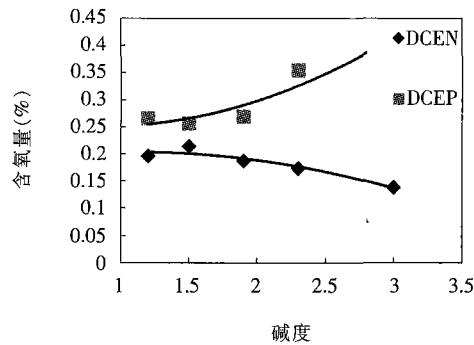


图5 直流正反接时过渡熔滴氧含量随碱度变化曲线

Fig.5 Oxygen content curves in traveling droplet with basicity index in DCEN and DCEP

3.3 碱度对熔滴金属氧含量的影响

根据图4、5直流正接和反接时焊丝末端熔化金属及激冷态过渡熔滴金属氧含量随碱度变化的曲线,可以看出正极性接法时,随着熔渣碱度的增大,熔滴金属氧含量是降低的,这与传统的熔渣碱度的热化学活性理论是相符的;然而该试验的一个有趣的结果是,在反极性条件下,随着熔渣碱度的增大,熔滴金属特别是图5中的过渡熔滴氧含量却呈上升变化,而且两种极性条件下氧含量差异随碱度的增大而增加。熔滴金属氧含量随熔渣碱度的增加而增大,这与传统熔渣碱度理论完全相反,但这种现象若用电化学观点则是可以解释的。众所周知,熔渣的离子理论将熔渣中自由氧离子的浓度定义为碱度,在低碱度的酸性熔渣中,氧离子往往形成复杂的链状复合离子团,从电极过程动力学上讲是不利于电化学作用的;反之具有较高氧离子活度的高碱度熔渣却是极其有利于电化学反应的。这说明高碱度在抑制熔渣/液态金属界面热化学作用方面虽是有效的,但在导致电化学作用方面却又是十分有利的。这种解释完全可以说明随着碱度的提高,正极性和反极性条件下熔滴金属氧含量之差异增大的试验结果。

试验结果表明,随着碱度的增大,碱度对熔滴阶段熔渣与液态熔滴热化学增氧的抑制作用有可能被电化学作用严重削弱,同时考虑到通常所采用的直流反极性条件下焊接时,熔滴生长阶段和熔池阶段在界面上的差异导致熔滴生长阶段界面电流密度远大于熔池阶段,其结果是熔滴阶段的电化学增氧程度远大于熔池阶段的脱氧程度。这说明高碱度熔渣在对熔滴金属电化学增氧问题上已占据了相当的地位,有可能成为增氧的主要机制,高碱度焊接材料的设计及直流焊接工艺的制定对此应有所考虑。

3.4 碱度对熔滴金属氮含量的影响

对过渡熔滴中氮含量变化的分析可以看出(图6所示),无论是电源极性还是碱度的大小,对

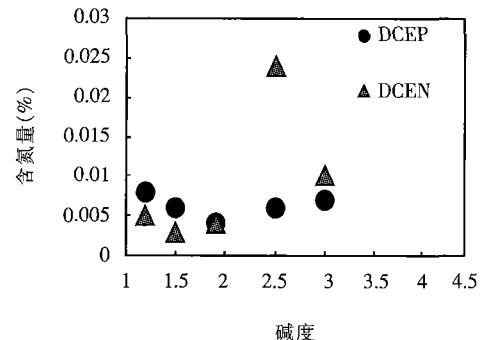


图6 直流正反接时过渡期溶滴氮含量与碱度关系

Fig.6 Nitrogen content curve of traveling droplet with basicity index in DCEN and DCEP

熔滴金属含氮量的影响并不呈现出规律性,并且数据相差不大。由于氮在熔渣或液态金属中不具备像氧那样的离子特性,因而并没有表现出氧那样的冶金电化学变化趋势,而仅取决于热化学作用的结果。这也从另一角度可以看出直流焊接时冶金电化学作用的效果是存在的。

4 结 论

(1) 直流 SAW 时,除传统的冶金热化学作用外,在焊接电弧的阴极和阳极熔渣与液态金属界面存在一定的冶金电化学作用,这种冶金电化学作用将对焊缝金属化学成分产生一定的影响。

(2) SAW 直流反极性焊接时生长期熔滴由于冶金电化学作用导致严重增氧;而正极性焊接时则导致脱氧。

(3) 碱度对直流 SAW 冶金电化学作用有着重要的影响,随着碱度的增加,冶金电化学作用愈加明显,因而对电化学致氧影响愈大,这在高碱度焊接材料的设计及焊接工艺的制订时有必要加以考虑。

参考文献:

- [1] Tuliani S S, Boniszewski T, Eatam N F. Notch toughness of commercial submerged arc weld metal [J]. Welding Metal Fab, 1969, (8): 327-339.
- [2] Lau T, Weatherly G C, Mclean A. Gas/metal slag reactions in submerged arc welding using CaO-Al₂O₃ based fluxes [J]. Welding Journal, 1986, 65(2): 31s-38s.

[上接第 8 页]

- spraying [J]. Transactions of the China Welding Institution, 2002, 23(1): 5-8.
- 朱子新, 梁秀兵, 徐滨士, 等. 高速电弧喷涂熔滴速度的数值模拟及试验研究 [J]. 焊接学报, 2002, 23(1): 5-8.
- [4] Zhu Zixin, Lu Yian, Xu Binshi, et al. Numerical analysis of heat transfer behavior of atomized droplets during high velocity spraying: I. mathematical model and variations of heat transfer parameters [J]. Transactions of the China Welding Institution, 2005, 26(1): 1-4, 8.
- 朱子新, 徐滨士, 马世宁, 等. 高速电弧喷涂 Fe-Al 合金熔滴传热过程数值模拟 I. 数学模型及传热参数变化规律 [J]. 焊接学报, 2005, 26(1): 1-4, 8.

- [3] Lau T, Weatherly G C, Mclean A. The sources of oxygen and nitrogen contamination in submerged arc welding using CaO-Al₂O₃ based fluxes [J]. Welding Journal, 1985, 64(12): 343s-347s.
- [4] Indacochea J E, Blander M, Shah S. Submerged arc welding: evidence for electrochemical effects on the weld pool [J]. Welding Journal, 1989, 68(3): 77s-83s.
- [5] Kim J H, Frost R H, Olson D L, et al. Effect of electrochemical reactions on submerged arc metal composition [J]. Welding Journal, 1990, 69(12): 446s-453s.
- [6] Polar A, Indacochea J E, Blander M. Electrochemically generated oxygen contamination in submerged arc welding [J]. Welding Journal, 1990, 69(2): 69s-74s.
- [7] Kim J H, Frost R H, Olson D L. Electrochemical oxygen transfer during direct current arc welding [J]. Welding Journal, 1998, 77(12): 488s-494s.
- [8] Olson D L, Edwards G R, Liu S, et al. Non-equilibrium behaviour of weld metal in flux-related processes [J]. Welding in the World, 1993, 31(2): 142-154.
- [9] Blander M, Olson D L. Electrochemical effects on weld pool chemistry in submerged arc and D. C. electroslag welding [A]. Proceedings of the international conference on the trends in welding research [C]. Gatlinburg Tenn, 1986, 363-366.
- [10] Frost R H, Olson D L, Edwards G R. The influence of electrochemical reactions on the chemistry of the electroslag welding process [C]. Proceedings of the Second Engineering Foundation Conference on Modeling of Casting and Welding Processes, 1983.
- [11] 李晓泉. SAW 熔渣/液态金属界面电化学现象 [J]. 焊接技术, 2003, 32(5): 6-8.

作者简介: 李晓泉,男,1964 年出生,副教授,博士研究生。主要从事焊接冶金及材料方向研究,承担多项基金项目及产、学、研项目。获省部级三等奖 1 项,发表论文 25 余篇。

Email: lxq2018@yahoo.com.cn

- [5] 莲井淳. 新版表面工学 [M]. 東京: 產報出版, 1996.
- [6] Steffens H D. Metallurgical changes in the arc spraying of steel [J]. British Welding Journal, 1966, 13(10): 597-605.
- [7] Sobolev V V, Guilemany J M. Dynamic processes during high velocity oxy fuel spraying [J]. International Materials Reviews, 1996, 41(1): 13-32.

作者简介: 朱子新,男,1968 年出生,工学博士,高级工程师,博士后研究人员。研究方向为防腐、耐磨新型热喷涂层的制备、结构与性能,发表论文 50 余篇。

Email: Zhuzx@eyou.com

MAIN TOPICS, ABSTRACTS & KEY WORDS

Numerical simulation of deep penetration in electron beam welding of Ti_3Al intermetallic compound WU Hui-qiang, FENG Ji-cai, HE Jing-shan, ZHANG Bing-gang (National Key Laboratory of Advanced Welding Production Technology, Harbin Institute of Technology, Harbin 150001, China). p1 - 4

Abstract: Three-dimensional quasi-steady temperature field numerical simulation of deep penetration in electron beam welding of Ti_3Al intermetallic compound was conducted on condition of moving heat source using modified double ellipsoidal mathematical model on basis of finite element method. In the model, the relationship between deep penetration and electron beam process parameter, material thermal physical properties and the convection and radiation effect, the latent heat of phase transformation, the temperature dependence of thermal physical properties and the convection heat transfer in the welding pool were considered. The simulation results showed a good agreement with the experimental results to confirm adaptability of the new model.

Key words: Ti_3Al ; electron beam welding; finite element; numerical simulation

Numerical analysis of heat transfer behavior of atomized droplets during high velocity arc spraying. II Influence of process parameters on heat transfer behavior of droplets ZHU Zi-xin^{1, 2}, LIU Yan¹, XU Bin-shi¹, Ma Shi-ning¹ (1. National Key Laboratory of Remanufacture, The Academy of Armored Forces Engineering, Beijing 100072; 2. Metrology Center of Aviation Equipments, Beijing 100070, China). p5 - 8, 12

Abstract: The influences of several important process parameters on the heat transfer behavior of the atomized droplets were numerically simulated and analyzed. The results show that the process parameters such as atomizing gas pressure, spraying current and spraying distance have great influences on the heat transfer behavior of the droplet. The droplet size considerably affects the heat transfer behavior of the atomized droplet. To a certain spraying distance, decreasing droplet size will increase the convective heat transfer coefficient, temperature and cooling rate, and decrease the solid fraction. Increasing atomizing gas pressure and spraying current will increase the droplet temperature and decrease the solid fraction to a certain spraying distance, and also extend the solidification process to a larger spray distance. The droplet cooling rate are much sensitive to the droplet size and spraying distance, but insensitive to the atomizing gas pressure and spraying current. The initial cooling rates of different size droplets range from 10^5 K/s to 10^7 K/s, thus producing the coating microstructure with the features of rapid solidification.

Key words: high velocity arc spraying; atomized droplet; heat transfer behavior; process parameter; numerical simulation

Effect of basicity index on electrochemically induced oxygen content

at droplet reaction stage in direct current submerged arc welding

LI Xiao-quan^{1, 2}, DU Ze-yu¹, LI Yun-tao¹, LIU Peng-fei², WANG Guang-yao² (1. Tianjin University, Tianjin 300072, China; 2. Jiangsu University of Science and Technology, Zhengjiang 212003, Jiangsu, China). p9 - 12

Abstract: Agglomerated fluxes with different basicity index were used in high-speed welding so as to attain rapid cooled droplet metal under two polarity conditions. The oxygen content of droplet metal was measured using oxygen-nitrogen instrument in order to analyze indirectly metallurgy electrochemical reaction occurred at interface between molten slag and liquid metal in cathode and anode of welding arc. The result showed that it is in the period of droplet growth at the tip of welding wire that an electrochemically gained oxygen was produced in the case of direct current negative polarity whereas an electrochemically lost oxygen in positive polarity. The slag basicity index has great influence upon metallurgy electrochemical reaction. With slag basicity index increasing, the effect of electrochemically induced oxygen which is contrary to thermochemical reaction become more evident for reacting dynamics depended on its ion characteristic and therefore it is necessary to be considered as an metallurgy factor.

Key words: basicity index; electrochemical reaction; submerged arc welding

Microstructure of particle reinforced Ni-base alloy composite coating by laser cladding LIU Shuo, ZHANG Wei-ping (Department of Materials Engineering, Dalian University of Technology, Dalian 116023, China). p13 - 16

Abstract: In-situ synthesis of TiB_2 ceramic particle reinforced Ni-base alloy composite coating has been conducted on 45 steel surface by CO_2 flow transverse laser. X-ray diffraction analysis shows γ -(Ni, Fe) solid-solution and ceramic phase mainly of TiB_2 in the coating. Scanning electron microscope, energy dispersive spectroscopy and electron probe microanalysis show that the dendrites dispersed homogeneously in the coating are very thin. The microstructure and composition in the dendrites are evidently different from that in the intergranular. The microstructure in the heat-affected zone is mainly composed of blended martensite. The microhardness of the coating increases substantially compared to that of the matrix.

Key words: laser cladding; particle reinforced; coating; microstructure

Formation mechanism of electron beam melt-brazed joint of chromium-bronze and duplex phase stainless steel ZHANG Bing-gang¹, FENG Ji-cai¹, WU Lin¹, LI Hong-wei¹, YANG Wei-peng², ZHU Chun-ling² (1. National Key Laboratory of Advanced Welding Production Technology, Harbin Institute of Technology, Harbin 150001, China; 2. Xi'an